

Fluid accretion onto relativistic stars and gravitational radiation

Alessandro Nagar^{1,2} and Guillermo Diaz²

¹*Università di Parma, Italy.*

²*Departament d'Astronomia i Astrofísica, Universitat de València, Spain.*

This article reports results from numerical simulations of the gravitational radiation emitted from nonrotating relativistic stars as a result of the axisymmetric accretion of layers of perfect fluid matter, shaped in the form of quadrupolar shells. We adopt a *hybrid* procedure where we evolve numerically the polar nonspherical perturbations equations of the star coupled to a fully nonlinear hydrodynamics code that calculates the motion of the accreting matter. Self-gravity of the accreting fluid as well as radiation reaction effects are neglected.

1 Introduction

In this article we shall report of the work made in collaboration with J.A. Pons and J.A. Font (see Ref. [1] for further details). The purpose is to analyze the gravitational wave emission pattern from neutron stars as a result of accretion of matter which is shaped in the form of quadrupolar shells. Accretion is expected to happen following the gravitational collapse of the core of a massive star, once a neutron star has already been formed. Part of the remaining stellar material which has not been expelled by the shock driving the supernova explosion may fall back onto the neutron star, until a critical mass is exceeded and the star collapses to a black hole. Some more material may in turn form a long-lived, centrifugally-supported torus or disk if the collapsing star had initially some amount of rotation [2]. A detailed realistic modelization of the gravitational emission from accretion flows would require three-dimensional (magneto-) hydrodynamical simulations in general relativity, coupled to radiation transport and diffusive processes. However, some preliminary steps can be taken to understand the underlying basic physics in a qualitative way. The procedure adopted here lies in the borderline of full numerical relativity and perturbation theory and extends to relativistic stars the 2D-axisymmetric computations concerned with black holes, formerly performed in Ref. [3]. The approach is as follows: the accreting matter, whose self-gravity is neglected, is evolved in a curved static background by solving the nonlinear hydrodynamics equations; the response of the star to the infalling matter, which triggers the emission of gravitational radiation, is computed by numerically solving the metric perturbations equations, with sources accounting

of the fluid motions. The key assumption of this method is that the mass of the accreting fluid is much smaller than that of the star, so that, fluid *self-gravity* as well as *radiation reaction* effects are neglected. The first approximation (no self-gravity) is in general valid for fluid motions in the vicinity of the star, where tidal forces dominate over the fluid self-gravity. The second approximation (no radiation reaction) is valid as long as the energy in the form of gravitational radiation is much smaller than the kinetic or internal energy of the fluid. We use then a particular implementation of the theory of metric perturbations of stars (see Ref. [4] and references therein for an extended description). A further simplification adopted is that the star is non rotating, so that metric, pressure, energy density and mass are obtained as solution of the Tolman-Oppenheimer-Volkoff equations of stellar equilibrium [5]. We assume barotropic equation of state written in polytropic form $p = K\epsilon^\Gamma$ to model a cold neutron star. We show results for two stellar models of mass $M = 1.4M_\odot$ with $\Gamma = 2$, the one being more compact than the other. The more compact model (A), has central density $\epsilon_c = 2.455 \times 10^{15} \text{ g/cm}^3$, and $K = 122.25 \text{ km}^2$, with $R = 9.80 \text{ km}$. The less compact model (B) has $\epsilon_c = 0.92 \times 10^{15} \text{ g/cm}^3$, and $K = 180 \text{ km}^2$ which leads to $R = 13.44 \text{ km}$.

2 Even-parity perturbations of a relativistic star

The presence of a fluid distribution outside the star creates a small perturbation in its gravitational field, so that the total metric is expressed as $g_{\mu\nu} = g_{\mu\nu}^0 + \delta g_{\mu\nu}$, where $g_{\mu\nu}^0$ is the metric of the star and $\delta g_{\mu\nu}$ is the perturbation; this can be decomposed in odd-parity (axial) and even-parity (polar) modes, each carrying spherical-harmonic indexes l and m [4]. Since the hydrodynamics evolution is 2D-axisymmetric ($\partial_\varphi = 0$) and because the star and the shell have no angular momentum, only the polar modes are excited by the accreting matter. For this reason we shall restrict the discussion below just to polar perturbations of stars. Formulations of the polar perturbations equations of a nonrotating stars suitable for time evolution are currently available in literature (see Ref. [1] and references therein). Our calculations are performed in the Regge-Wheeler gauge [8], by specializing the gauge-invariant and coordinate independent formalism of Ref. [9]. The equations obtained are equivalent to those of Ref. [6] and [7], although different metric variables are used. Thus, for each (l, m) pair, $\delta g_{\mu\nu}$ is parametrized by two scalar quantities, k (the perturbed 3-conformal factor) and χ (the actual gravitational wave degree of freedom), and it reads

$$\delta g_{\mu\nu} dx^\mu dx^\nu = [(\chi + k)e^{2a} dt^2 - 2\psi e^{a+b} dt dr + (\chi + k)e^{2b} dr^2 + kr^2 d\Omega^2] Y^{\ell m} . \quad (1)$$

On a static background ψ does not play any dynamical role, as it can be obtained by quadrature from k and χ [9]. We note that, despite this problem has actually two

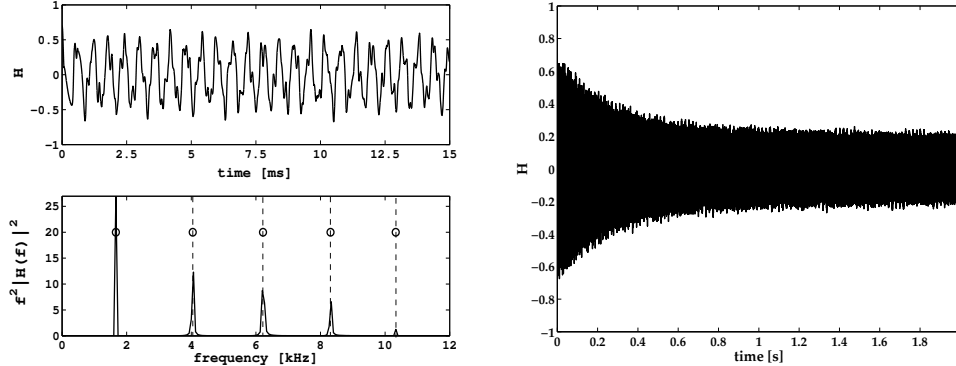


Figure 1: Time evolution of the enthalpy perturbation of model B

degrees of freedom inside the star and one outside it, we have found more convenient for numerical reasons to consider an additional variable inside the star, the perturbation of the relativistic enthalpy $H = \delta p / (p + \epsilon)$. We are left, then, with three degrees of freedom inside the star (χ , k and H) and two outside (χ and k). Outside the star, from k and χ we get the Zerilli-Moncrief function [10, 11]

$$Z = \frac{4r^2 e^{-2b}}{\lambda[(\lambda - 2)r + 6M]} \left[\chi + \left(\frac{\lambda}{2} + \frac{M}{r} \right) e^{2b} k - r k_{,r} \right], \quad (2)$$

with $\lambda = l(l + 1)$, whose Fourier transform gives the energy radiated in GWs

$$E^{\ell m} = \frac{\pi}{8} \frac{(l + 2)!}{(l - 2)!} \int_0^\infty f^2 \left| \tilde{Z}(f, r) \right|^2 df. \quad (3)$$

Unlike other studies [6, 7], we choose to evolve the perturbations through a couple of hyperbolic equations for χ and H plus an elliptic equation, the Hamiltonian constraint, which is solved for k at every temporal slice. With this “constrained” scheme, that works as a dynamical corrector of the truncation errors, we gain two important benefits: on one hand we can obtain the frequencies of the fluid modes (by Fourier transforming the waveforms) with very good accuracy even with a relatively low resolution; on the other hand, we do not have limits to the evolution time (unlike free hyperbolic formulations, where sooner or later a violation of the constraints occurs and the evolution must be stopped), and we can see dynamically the damping of the fluid modes due to GWs emission. Fig. 1 shows the evolution of an initial enthalpy profile as $H = \sin(\pi r / 2R)$ for model B, observed at half of the star radius. The circles in the Fourier spectrum represent the fluid modes obtained using a frequency-domain code based on the Lindblom-Detweiler formulation of the

perturbed equations [12] and described in [13]. The relative difference between the location of the peaks and these values is of some parts in a thousand, with a resolution of 200 points. The right panel of Fig. 1 refers to the same evolution carried out for 2 s. The damping time of the f -mode for this model is $\tau_f = 0.26$ s: after ~ 1 s just the longer living p -modes survive in the signal [4].

3 Gravitational waves from fluid accretion

We present an overview of a typical simulation of accretion onto model A. Initially, the non spherical density profile is surrounded by a background fluid (an “atmosphere”) satisfying the stationary and spherically symmetric Michel solution [14]. The initial rest mass density profile is given by

$$\rho = \rho_{\text{Mich}} + \rho_{\text{max}} e^{-\kappa(r-r_0)^2} \sin^2 \vartheta , \quad (4)$$

with ρ_{Mich} being the profile consistent with the Michel solution. The mass of the shell is $\mu = 0.01M$, which corresponds to a maximum density of $\rho_{\text{max}} \sim 3.5 \times 10^{-6} \text{ km}^{-2}$ when we fix its width to $\kappa = 1$. The (inhomogeneous) density profile of the atmosphere ρ_{Mich} is roughly three orders of magnitude lower than ρ_{max} . The shell obeys a polytropic ($p = \mathcal{K}\rho^\gamma$) EoS with $\mathcal{K} = 0.01 \text{ km}^{2/3}$ and $\gamma = 4/3$. The internal energy profile is obtained from the baryonic density ρ and p through the first law of thermodynamics as $e = p/((\gamma - 1)\rho)$. The shell is initially at rest at $r_0 = 20$ km, and the waveform is extracted at $r_{\text{obs}} = 250$ km.

The motion of the fluid in a curved spacetime is governed by the local conservation laws of baryonic number and energy-momentum; as shown by [15], the equations of general relativistic hydrodynamics can be written as a hyperbolic system of balance laws with sources, and then solved using a Godunov-type scheme based on the characteristic information of the system. The hydrodynamics code employed here is the same of Ref. [3].

In a realistic scenario, such as e.g. fall-back accretion after a supernova explosion, the accreting matter interacts with the neutron star until a critical mass is reached and the star collapses to a black hole. As we cannot model this complex phenomenon within the current perturbative framework, we impose reflecting boundary conditions at the inner edge of the hydrodynamics domain (i.e. the surface of the star), so that it is seen by the external fluid as a *hard* sphere. This choice includes the most relevant effect, that is, the pressure gradient stops the infalling matter, and the accretion process is then followed by the formation of shock waves which propagate off the stellar surface. The impact of the shell perturbs the star and triggers its quasinormal modes of pulsation, so that it radiates gravitational waves.

Fig. 2 exhibits the time evolution of the Zerilli-Moncrief function and the corresponding energy spectrum. In the waveforms, three phases can be identified. Firstly,

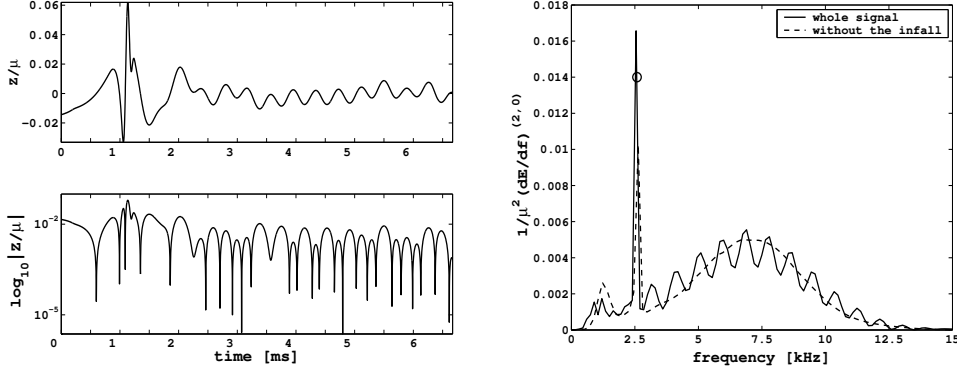


Figure 2: Waveform and energy spectra from a fluid shell falling on to star model A.

the infalling, when the bulk of the shell is evolving outside the star, gradually approaching it, which is characterized by the steady increase of the amplitude of the signal: it is very short as the shell is initially located very close to the stellar surface. Secondly, a burst-like peak appears in the GW signal, which, as found in simulations of gravitational core collapse [16], coincides with the moment when the shell reaches the surface, creating a shock wave which propagates off the surface. Finally, the ring-down phase, characterized by a GW signal which is not exactly monochromatic as a result of the complex interaction between the gravitational field of the star and the layers of fluid captured on top of the stellar surface in the process of readjusting themselves to a new stationary solution. We note that, despite a remarkable resemblance with the results of core collapse simulations [16], there are also important differences in the post-bounce phase dynamics, as the ringdown of the neutron star lasts for much longer times. In our idealized setup these pulsations are not quickly damped by the existence of a dense envelope surrounding the star, as happens in the core collapse situation. Concerning the energy spectra, the solid line is obtained by Fourier transforming the complete signal; correspondingly, the dashed line comes from the truncated waveform, in which we only take into account the contribution from the beginning of the burst (~ 0.9 ms) onward. The whole spectrum shows a complex structure: first of all, we find a narrow peak, identified with the f -mode of the star with an error around 1%. At higher frequencies, we have a broad band spectrum modulated by roughly equally spaced bumps ($\delta f \approx 0.9$ kHz). These are interference effects coming from the pre-bounce phase of the emission. This is confirmed by the fact that they are absent in the truncated spectrum. This latter presents one broad peak with a maximum at about 7 kHz, which is however too low to be identified with the w -mode. As mentioned before, its origin should be related to the motion of

the fluid shell and its interference with the gravitational field of the star: the high-frequency emission depends, then, on details of the dynamics of accretion rather than on intrinsic characteristics of the star. The total energy emitted in this process is computed by integrating the spectrum of Fig. 2. We get $E^{20} \simeq 3.02 \times 10^{-8} M_{\odot} c^2$ or, in terms of the shell mass, $E^{20} \simeq 2.15 \times 10^{-6} \mu c^2$.

As a last remark, we note that a small amplitude peak, at frequency lower than that of the f -mode, is present in the spectrum. It is associated with oscillations of that part of the external fluid that has been gravitationally captured by the star as a result of accretion. We argue that the existence of this unphysical low frequency peak is an artifact produced by the reflecting boundary conditions imposed at the surface. In a realistic scenario, the accreted matter would not simply bounce at the stellar surface, but it would rather interact with the neutron star envelope, resulting in heating and suffering nuclear reactions, until it is reabsorbed by the star.

References

- [1] A. Nagar, G. Diaz, J. A. Pons, J. A. Font, Phys. Rev. D **69**, 124028 (2004).
- [2] J.A. Font and F. Daigne, Astrophys. J. Lett. **581**, L23 (2004).
- [3] P. Papadopoulos and J.A. Font, Phys. Rev. D **59**, 044014 (1999).
- [4] K.D. Kokkotas and B.G. Schmidt, *Quasi Normal Modes of Stars and Black Holes*, www.livingreviews.org/Articles/Volume2/1999-2kokkotas.
- [5] C.W. Misner, K.S. Thorne, and J.A. Wheeler, *Gravitation*, Freeman and Company, New York (1973).
- [6] G. Allen, N. Andersson, K.D. Kokkotas, and B.F. Schutz, Phys. Rev. D **58**, 124012 (1998).
- [7] J. Ruoff, Phys. Rev. D **63**, 064018 (2001).
- [8] T. Regge and J.A. Wheeler, Phys. Rev. **108**, 1063 (1957).
- [9] C. Gundlach and J.M. Martín-García, Phys. Rev. D **61**, 084024 (2000); *ibid.* **64**, 024012 (2001).
- [10] F.J. Zerilli, Phys. Rev. D **2**, 2141 (1970).
- [11] V. Moncrief, Ann. Phys. (N.Y.) **88**, 323 (1974).
- [12] L. Lindblom and S.L. Detweiler, Astrophys. J. Suppl., **53**, 73 (1983); S.L. Detweiler and L. Lindblom, Astrophys. J. **292**, 12-15 (1985).
- [13] J.A. Pons, E. Berti, L. Gualtieri, G. Miniutti, and V. Ferrari, Phys. Rev. D **65**, 104021 (2002).
- [14] F.C. Michel, Astrophys. Space Sci. **15**, 153 (1972).
- [15] F. Banyuls, J.A. Font, J.M. Ibáñez, J.M. Martí, and J.A. Miralles, Astrophys. J. **476**, 221 (1997).
- [16] H. Dimmelmeier, J.A. Font, and E. Müller, Astron. Astrophys. **393**, 523 (2002).